A REDUCED BASIS METHOD FOR PARAMETRIZED VARIATIONAL INEQUALITIES[*]

B. HAASDONK[†], J. SALOMON[‡], AND B. WOHLMUTH[§]

Abstract. Reduced basis methods are an efficient tool for significantly reducing the computational complexity of solving parametrized PDEs. Originally introduced for elliptic equations, they have been generalized during the last decade to various types of elliptic, parabolic, and hyperbolic systems. In this article, we extend the reduction technique to parametrized variational inequalities. First, we propose a reduced basis variational inequality scheme in a saddle point form and prove existence and uniqueness of the solution. We state some elementary analytical properties of the scheme such as reproduction of solutions, a priori stability with respect to the data, and Lipschitz-continuity with respect to the parameters. An offline/online decomposition guarantees an efficient assembling of the reduced scheme, which can be solved by constrained quadratic programming. Second, we provide rigorous a posteriori error bounds with a partial offline/online decomposition. The reduction scheme is applied to one-dimensional obstacle problems. The numerical results confirm the theoretical ones and demonstrate the efficiency of the reduction technique.

Key words. model reduction, reduced basis methods, variational inequalities, a posteriori error bounds

AMS subject classifications. 35J86, 65K15, 65N12, 65N15

DOI. 10.1137/110835372

1. Introduction. We consider efficient solution strategies for parametrized variational inequalities. Such problems can be obtained from variational formulations with additional constraints and play an important role in many applications. For any given parameter $\boldsymbol{\mu} \in \mathcal{P} \subset \mathbb{R}^p$ we are interested in finding a solution $u(\boldsymbol{\mu})$ of the following minimization problem:

$$(1.1) \qquad \min_{u \in X(\boldsymbol{\mu})} \frac{1}{2} a(u, u; \boldsymbol{\mu}) - f(u; \boldsymbol{\mu})$$

with $X(\boldsymbol{\mu}) \subseteq V$ a closed convex nonempty set in a separable Hilbert space V, $a(\cdot, \cdot; \boldsymbol{\mu})$ a symmetric, continuous, and coercive bilinear form, and $f(\cdot; \boldsymbol{\mu})$ a continuous linear form. For $X(\boldsymbol{\mu}) = V$ the above is a standard unconstrained optimization problem. Then, the first order optimality condition yields a simple linear system of equations for the solution $u(\boldsymbol{\mu})$. However, if $X(\boldsymbol{\mu})$ is a proper convex subset of V, the solution cannot be obtained from a simple linear system of equations. Quite often, the convex set can be characterized in terms of a dual cone M. Then (1.1) can be reformulated as a saddle point formulation which can be solved by primal-dual active set methods. For a background on variational optimization with constraints and some applications, we refer the reader to the monographs [8, 9, 14, 16] and the references therein. Assume now that the above problem must be solved in a multiquery or real-time context;

i.e., the computation of the solution is required to be extremely fast and/or has to be done for many parameters. For standard PDEs in variational form, reduced basis methods [2, 22] provide efficient tools for problem-specific dimensionality reduction. More precisely, instead of the full problem, which is typically infinite or rather high-dimensional, a low-dimensional model is generated which can consequently be solved significantly faster for varying parameters. Many types of PDEs have been treated by this reduction technique during the last decade ranging from elliptic [22] to parabolic [10, 20] and hyperbolic equations [12]. So far, all results are restricted to equation systems and no additional inequality constraints are taken into account. We are interested in adapting these techniques to a class of variational inequality problems. We will reformulate our variational inequality as a saddle point problem that has some components similar to those of the Stokes system which has already been successfully treated with reduced basis methods; see, e.g., [17, 19, 21, 23]. We refer the reader to [5, 18] for an abstract saddle point theory and the important role of the supremizer operator.

This article is structured as follows. In the next section, we give the elementary notation and definitions of the full and reduced problem in a saddle point formulation, its discrete formulation, and an offline/online decomposition. In section 3, we show consistency, boundedness with respect to the data, and Lipschitz-continuity with respect to the parameter. Section 4 is devoted to rigorous a posteriori error estimation based on equality and inequality residuals. However, due to the nonlinear nature of the inequality, we can currently provide only an incomplete offline/online decomposition for these error estimators. In section 5, we comment on various computational aspects for finite element discretizations with biorthogonal dual bases for the constraints. Finally, in section 6, we consider as a model problem a one-dimensional obstacle-type inequality. Numerical results illustrate the performance of the proposed method.

2. Reduced basis (RB) approximation of a variational inequality. This section is devoted to the derivation of a general RB formulation for a standard variational inequality.

2.1. Notation. We briefly introduce the notation and assumptions which will be used throughout the paper. By V, W we denote two separable Hilbert spaces with inner products $\langle \cdot, \cdot \rangle_V$, $\langle \cdot, \cdot \rangle_W$ and induced norms $\|\cdot\|_V$, $\|\cdot\|_W$. The set $M \subset W$ is assumed to be a closed, nonempty, convex cone. We assume $a(\cdot, \cdot; \boldsymbol{\mu})$ to be a uniformly continuous symmetric and coercive bilinear form on $V \times V$ for all $\boldsymbol{\mu} \in \mathcal{P}$, where $\mathcal{P} \subset \mathbb{R}^p$, $p \in \mathbb{N}$, is the parameter domain. More precisely, the parameter-dependent coercivity $\alpha(\boldsymbol{\mu})$ and continuity $\gamma_a(\boldsymbol{\mu})$ constants can be bounded for all $\boldsymbol{\mu} \in \mathcal{P}$ by $0 < \bar{\alpha} \leq \alpha(\boldsymbol{\mu})$ and $\gamma_a(\boldsymbol{\mu}) \leq \bar{\gamma}_a < \infty$, respectively. Moreover, we assume that $a(\cdot, \cdot; \boldsymbol{\mu})$ is Lipschitz-continuous with respect to $\boldsymbol{\mu}$; i.e., for a suitable constant $L_a > 0$ we have $|a(u, v; \boldsymbol{\mu}) - a(u, v; \boldsymbol{\mu}')| \leq L_a \|u\|_V \|v\|_V \|\boldsymbol{\mu} - \boldsymbol{\mu}'\|$ for all $\boldsymbol{\mu}, \boldsymbol{\mu}' \in \mathcal{P}, u, v \in V$. Here $\| \cdot \|$ denotes a norm on $\mathbb{R}^p$, e.g., the Euclidean norm. We assume that the parameter-dependent linear forms $f(\cdot; \boldsymbol{\mu}) \in V'$, $g(\cdot; \boldsymbol{\mu}) \in W'$ are uniformly continuous in $\boldsymbol{\mu}$; i.e., there exist constants $\bar{\gamma}_f, \bar{\gamma}_g > 0$ with $\|f(\cdot; \boldsymbol{\mu})\|_{V'} \leq \bar{\gamma}_f$ and $\|g(\cdot; \boldsymbol{\mu})\|_{W'} \leq \bar{\gamma}_g$ for all $\boldsymbol{\mu} \in \mathcal{P}$. Furthermore, $f(\cdot; \boldsymbol{\mu})$ and $g(\cdot; \boldsymbol{\mu})$ are supposed to be Lipschitz-continuous with respect to $\boldsymbol{\mu}$; i.e., for suitable constants $L_f, L_g > 0$ it holds that $\|f(\cdot; \boldsymbol{\mu}) - f(\cdot; \boldsymbol{\mu}')\|_{V'} \leq L_f \|\boldsymbol{\mu} - \boldsymbol{\mu}'\|$ and $\|g(\cdot; \boldsymbol{\mu}) - g(\cdot; \boldsymbol{\mu}')\|_{W'} \leq L_g \|\boldsymbol{\mu} - \boldsymbol{\mu}'\|$ for all $\boldsymbol{\mu}, \boldsymbol{\mu}' \in \mathcal{P}$. Finally, $b(\cdot, \cdot)$ stands for a continuous bilinear form on $V \times W$ with continuity constant $\gamma_b > 0$, which is inf-sup stable; i.e., there exists $\beta > 0$ such that $\inf_{\eta \in W} \sup_{v \in V} b(v, \eta)/(\|v\|_V \|\eta\|_W) \geq \beta$. We assume a separable parameter dependence in $a(\cdot, \cdot; \boldsymbol{\mu})$, $f(\cdot; \boldsymbol{\mu})$, and $g(\cdot; \boldsymbol{\mu})$, i.e., the existence of parameter-dependent

scalar functions $\theta_a^q, \theta_f^q, \theta_g^q : \mathcal{P} \to \mathbb{R}$, and of parameter-independent components, i.e., continuous symmetric bilinear forms $a^q(\cdot, \cdot)$ and linear functionals $f^q(\cdot) \in V'$, $g^q(\cdot) \in W'$, such that $a(u, v; \boldsymbol{\mu}) = \sum_{q=1}^{Q_a} \theta_a^q(\boldsymbol{\mu}) a^q(u, v)$, and similar expansions for f and g, preferably with small $Q_a, Q_f, Q_g \in \mathbb{N}$.

2.2. Detailed problem definition. From now on, we assume that the convex set $X(\boldsymbol{\mu})$ can be defined in terms of the convex cone M and the linear form $g(\cdot; \boldsymbol{\mu})$, i.e., $X(\boldsymbol{\mu}) = \{v \in V | b(v, \eta) \leq g(\eta; \boldsymbol{\mu}), \eta \in M\}$. Then (1.1) is equivalent to a saddle point problem.

DEFINITION 2.1 (variational saddle point problem $SP(\boldsymbol{\mu})$).

Given $\boldsymbol{\mu} \in \mathcal{P}$, find $(u(\boldsymbol{\mu}), \lambda(\boldsymbol{\mu})) \in V \times M$ such that

$$a(u(\boldsymbol{\mu}), v; \boldsymbol{\mu}) + b(v, \lambda(\boldsymbol{\mu})) = f(v; \boldsymbol{\mu}), \qquad v \in V,$$
$$b(u(\boldsymbol{\mu}), \eta - \lambda(\boldsymbol{\mu})) \leq g(\eta - \lambda(\boldsymbol{\mu}); \boldsymbol{\mu}), \quad \eta \in M.$$

The proofs of existence and uniqueness are well known; see, e.g., [9]. A notable and frequently used property of the solution $(u(\boldsymbol{\mu}), \lambda(\boldsymbol{\mu}))$ is

$$(2.1) \qquad\qquad b(u(\boldsymbol{\mu}), \lambda(\boldsymbol{\mu})) = g(\lambda(\boldsymbol{\mu}); \boldsymbol{\mu}),$$

which is obtained by using $\eta = 0$ and $\eta = 2\lambda(\boldsymbol{\mu})$ as test functions in $SP(\boldsymbol{\mu})$. Note that the problem $SP(\boldsymbol{\mu})$ can be the analytical problem in infinite-dimensional spaces or the discretized problem in finite-dimensional spaces of high dimension. In the case of finite-dimensional spaces $V = \text{span}\{\psi_i, i = 1, \ldots, H_V\}$ and $W = \text{span}\{\chi_i, i = 1, \ldots, H_W\}$, we denote by H_V and H_W the dimension of V and W, respectively. In our numerical tests, we use conforming finite elements for V and for W having the same dimension $H := H_V = H_W$.

As we will see, the case $Q_a = 1$ is of special interest. In that situation, we have $a(u, v; \boldsymbol{\mu}) = \theta_a^1(\boldsymbol{\mu}) a^1(u, v)$ with $\theta_a^1(\boldsymbol{\mu}) \geq \theta_{min} > 0$ and $a^1(\cdot, \cdot)$ being symmetric and coercive. By dividing the first equation of $SP(\boldsymbol{\mu})$ with $\theta_a^1(\boldsymbol{\mu})$ we obtain an equivalent problem with nonparametric $a(\cdot, \cdot)$ and correspondingly scaled $f(\cdot; \boldsymbol{\mu})$ and $\lambda(\boldsymbol{\mu})$. Hence, for the analysis of the case $Q_a = 1$ we can always assume without loss of generality that $a(\cdot, \cdot)$ and therefore α, γ_a are nonparametric. Recall that $b(\cdot, \cdot)$ is nonparametric by definition. We introduce the operators $A : V' \to V$, $B : W \to V$, and $C : W \to V$ by

$$a(A\ell, v) := \ell(v), \qquad \langle B\eta, v \rangle_V := b(v, \eta), \qquad a(C\eta, v) := b(v, \eta), \quad v \in V, \eta \in W.$$

2.3. Reduced problem definition. We now derive from the saddle point formulation of Definition 2.1 a corresponding RB method. Let $S = \{\boldsymbol{\mu}_1, \ldots, \boldsymbol{\mu}_{N_S}\} \subset \mathcal{P}$ denote a finite parameter sample set of N_S parameters and $(u(\boldsymbol{\mu}_i), \lambda(\boldsymbol{\mu}_i)) \in V \times M$ the corresponding solutions of $SP(\boldsymbol{\mu}_i)$, the so-called *snapshots*. We consider different choices of a reduced dual space $W_N := \text{span}\{\xi_i\}_{i=1}^{N_W}$ and reduced closed convex cone $M_N := \text{span}_+\{\xi_i\} := \{\sum_{i=1}^{N_W} \alpha_i \xi_i | \alpha_i \geq 0\}$:

1. Pure dual snapshots: We identify $\xi_i := \lambda(\boldsymbol{\mu}_i)$ and set

$$(2.2) \qquad\qquad W_N^{(1)} := \text{span}\{\lambda(\boldsymbol{\mu}_i)\}_{i=1}^{N_S}.$$

2. Detailed basis subset: We assume that the detailed cone is spanned by the χ_j, i.e., $M = \text{span}_+\{\chi_j\}_{j=1}^{H_W}$. We define $J \subset \{1, \ldots, H_W\}$ to be the smallest subset satisfying $\lambda(\boldsymbol{\mu}_i) \in \text{span}_+\{\chi_j\}_{j \in J}$ for all $i = 1, \ldots, N_S$. Then we set $\{\xi_i\}_{i=1}^{N_W} := \{\chi_j\}_{j \in J}$ and

$$(2.3) \qquad\qquad W_N^{(2)} := \text{span}\{\chi_j\}_{j \in J}.$$

It can easily be verified that with these choices $\lambda(\boldsymbol{\mu}_i) \in M_N$ and $\xi_i \in M$ and hence $M_N \subset M$. Note that we do not explicitly require linear independence of the $\{\xi_i\}$, but also accept a possibly linearly dependent family. In this case, elements $\eta \in M_N$ may have multiple different equivalent expansions as a linear combination of $\{\xi_i\}$. The number of coefficients N_W is the relevant quantity for computational complexities. We have $\dim W_N \leq N_W$; in the case of $W_N^{(1)}$ we observe $N_W = N_S$ and in the case of $W_N^{(2)}$ we will most likely have $N_W \geq N_S$.

Remark 2.2. Note that the choice $W_N^{(2)}$ is reasonable only for problems where the dual snapshots are expected to have a small domain of support. For example, in case $N_S = 1$ and a single dual multiplier $\lambda(\boldsymbol{\mu}_1)$ of global support, we obtain $W_N^{(2)} = W$ and hence $N_W = H_W$, which certainly cannot be considered as being "reduced." The set J can simply be found as the union of all indices of nonzero degrees of freedom of the dual snapshots.

For formulating the reduced scheme, it remains to give a definition of the reduced space V_N for the primal variable. For this space, we also consider different choices:

1. Pure primal snapshots: The naive choice for the reduced primal space is given by

$$(2.4) \qquad\qquad V_N^{(1)} := \mathrm{span}\{u(\boldsymbol{\mu}_i)\}_{i=1}^{N_S} \subset V.$$

2. Enrichment by supremizers: This choice is motivated by [21]

$$(2.5) \qquad\qquad V_N^{(2)} := \mathrm{span}\{u(\boldsymbol{\mu}_i), B\xi_j\}_{i,j=1}^{N_S, N_W} \subset V.$$

3. Enrichment by a priori solutions: If $Q_a = 1$, an attractive alternative option is

$$(2.6) \qquad\qquad V_N^{(3)} := \mathrm{span}\{u(\boldsymbol{\mu}_i), Af^q\}_{i,q=1}^{N_S, Q_f} \subset V.$$

4. Enrichment by unconstrained solutions: If $Q_a = 1$, we can also set

$$(2.7) \qquad\qquad V_N^{(4)} := \mathrm{span}\{u(\boldsymbol{\mu}_i), Af(\cdot; \boldsymbol{\mu}_i)\}_{i=1}^{N_S} \subset V.$$

We quite often neglect the upper index (l), $l = 1, 2, 3, 4$, set $N_V := \dim V_N$, and denote the basis of V_N by $\{\varphi_i\}_{i=1}^{N_V}$. We point out that the subscript N does not stand for the dimension but indicates only that the quantity is connected to a *reduced* problem. In the following, we use some further notation: given an element w, we denote its coefficient vectors by $\overline{w}$ when dealing with the reduced basis and by $\underline{w}$ when considering its representation in the high (finite-)dimensional spaces. Moreover, from time to time, we omit the $\boldsymbol{\mu}$-dependence.

The goal of an RB scheme is the computation of parameter-dependent solutions $u_N(\boldsymbol{\mu}) \in V_N, \lambda_N(\boldsymbol{\mu}) \in M_N$ by solving a saddle point problem of low complexity.

DEFINITION 2.3 (reduced basis saddle point problem $SP_N(\boldsymbol{\mu})$).
For $\boldsymbol{\mu} \in \mathcal{P}$ find $(u_N(\boldsymbol{\mu}), \lambda_N(\boldsymbol{\mu})) \in V_N \times M_N$ such that

$$a(u_N(\boldsymbol{\mu}), v_N; \boldsymbol{\mu}) + b(v_N, \lambda_N(\boldsymbol{\mu})) = f(v_N; \boldsymbol{\mu}), \quad v_N \in V_N,$$
$$b(u_N(\boldsymbol{\mu}), \eta_N - \lambda_N(\boldsymbol{\mu})) \leq g(\eta_N - \lambda_N(\boldsymbol{\mu}); \boldsymbol{\mu}), \quad \eta_N \in M_N.$$

The following proposition shows that the pairing (V_N, W_N) inherits its inf-sup constant from the pairing (V, W), and thus $SP_N(\boldsymbol{\mu})$ has a unique solution for $V_N = V_N^{(i)}$, $i = 2, 3, 4$.

PROPOSITION 2.4 (existence and uniqueness of $SP_N(\boldsymbol{\mu})$). *Pairings* $(V_N^{(2)}, W_N^{(1)})$, $(V_N^{(2)}, W_N^{(2)})$ *are inf-sup stable with* $\beta_N \geq \beta$, *and* $(V_N^{(3)}, W_N^{(1)})$, $(V_N^{(4)}, W_N^{(1)})$ *are inf-sup stable with* $\beta_N \geq \beta\sqrt{\alpha/\gamma_a}$. *Thus existence and uniqueness are guaranteed.*

Proof. The case $V_N = V_N^{(2)}$ is a special case of Lemma 3.1 in [23], here with a nonparametric form $b(\cdot, \cdot)$. If $Q_a = 1$, we assume without loss of generality (w.l.o.g.) that $a(\cdot, \cdot)$ is nonparametric and obtain by the fact that $(u(\boldsymbol{\mu}_i), \lambda(\boldsymbol{\mu}_i))$ solves $SP(\boldsymbol{\mu}_i)$

$$a(C\lambda(\boldsymbol{\mu}_i), v) = b(v, \lambda(\boldsymbol{\mu}_i)) = f(v; \boldsymbol{\mu}_i) - a(u(\boldsymbol{\mu}_i), v).$$

Then, the definition of the operators yields

$$C\lambda(\boldsymbol{\mu}_i) = Af(\cdot; \boldsymbol{\mu}_i) - u(\boldsymbol{\mu}_i).$$

By linearity, this implies that $C\eta_N \in V_N^{(i)}$, $i = 3, 4$, for all $\eta_N \in W_N$. Using the norm equivalence on V gives by a straightforward computation

$$
\begin{aligned}
\beta_N &:= \inf_{\eta_N \in W_N} \sup_{v_N \in V_N} \frac{b(v_N, \eta_N)}{\|v_N\|_V \|\eta_N\|_W} = \inf_{\eta_N \in W_N} \sup_{v_N \in V_N} \frac{a(v_N, C\eta_N)}{\|v_N\|_V \|\eta_N\|_W} \\
&\geq \inf_{\eta_N \in W_N} \sup_{v_N \in V_N} \frac{\sqrt{\alpha} a(v_N, C\eta_N)}{\sqrt{a(v_N, v_N)} \|\eta_N\|_W} = \inf_{\eta_N \in W_N} \frac{\sqrt{\alpha} a(C\eta_N, C\eta_N)}{\sqrt{a(C\eta_N, C\eta_N)} \|\eta_N\|_W} \\
&= \sqrt{\alpha} \inf_{\eta_N \in W_N} \sup_{v \in V} \frac{a(v, C\eta_N)}{\sqrt{a(v, v)} \|\eta_N\|_W} \geq \frac{\sqrt{\alpha}}{\sqrt{\gamma_a}} \inf_{\eta_N \in W_N} \sup_{v \in V} \frac{b(v, \eta_N)}{\|v\|_V \|\eta_N\|_W} \geq \frac{\sqrt{\alpha}}{\sqrt{\gamma_a}} \beta. \quad \square
\end{aligned}
$$

No stability statement can be given for the choice $V_N^{(1)}$ in (2.4). One can even explicitly construct pathological cases, where the uniqueness is not valid: Assume a simple example of $N_S = 1$, $\boldsymbol{\mu}_1 \in \mathcal{P}$, and $g(\cdot; \boldsymbol{\mu}_1) = 0$. Then, the solutions $u(\boldsymbol{\mu}_1), \lambda(\boldsymbol{\mu}_1)$ are b-orthogonal, i.e., $b(u(\boldsymbol{\mu}_1), \lambda(\boldsymbol{\mu}_1)) = 0$, which is obtained from (2.1). If we assume a definition of reduced spaces without supremizer, i.e., $V_N := \mathrm{span}\{u(\boldsymbol{\mu}_1)\}$, $M_N := \{s\lambda(\boldsymbol{\mu}_1), s \in \mathbb{R}_0^+\} \subset W_N := \mathrm{span}\{\lambda(\boldsymbol{\mu}_1)\}$, this implies two conceptual problems: First, the solution $u_N(\boldsymbol{\mu}_1)$ of $SP_N(\boldsymbol{\mu})$ is not constrained in any way, and hence we solve an ordinary unconstrained PDE. Second, we lose the uniqueness of solutions, due to the lack of the inf-sup stability. Any $(u_N, \lambda_N) := (u(\boldsymbol{\mu}_1), s\lambda(\boldsymbol{\mu}_1))$ for $s \in \mathbb{R}_0^+$ is a solution of $SP_N(\boldsymbol{\mu}_1)$. Still, in practice the choice (2.4) may lead to an inf-sup stable and very accurate scheme, but the inf-sup stability constants can possibly be arbitrarily small.

Remark 2.5. If $Q_a = 1$, the choices (2.6) and (2.7) are possibly computationally attractive alternatives to (2.5). First, in the case of $N_W \gg Q_f$, the Q_f a priori solutions for the enrichment in (2.6) are considerably less costly than the N_W supremizer functions in (2.5). Second, the constrained solution is often calculated in terms of an iterative solver which uses as initial guess the solution $Af(\cdot; \boldsymbol{\mu}_i)$ of the unconstrained system. Thus no additional cost at all is then required in (2.7). We highlight some interesting relations between the $V_N^{(i)}$: It is easy to see that $Af(\cdot; \boldsymbol{\mu}_i) = \sum_{q=1}^{Q_f} \theta_f^q(\boldsymbol{\mu}_i) Af^q \in V^{(3)}$ and thus $V_N^{(4)} \subseteq V_N^{(3)}$. Equality holds as soon as $V_N^{(4)}$ is rich enough, i.e., $\dim(\mathrm{span}(Af(\cdot; \boldsymbol{\mu}_i)_{i=1}^{N_S})) = Q_f$. Moreover, if additionally $a(\cdot, \cdot) = \langle \cdot, \cdot \rangle_V$, then $SP(\boldsymbol{\mu}_i)$ yields

$$\langle B\lambda(\boldsymbol{\mu}_i), v \rangle_V = b(v, \lambda(\boldsymbol{\mu}_i)) = f(v; \boldsymbol{\mu}_i) - a(u(\boldsymbol{\mu}_i), v) = \langle Af(\cdot; \boldsymbol{\mu}_i) - u(\boldsymbol{\mu}_i), v \rangle_V$$

and thus $V_N^{(2)} \subseteq V_N^{(4)}$, and the dimension of $V_N^{(2)}$ is at most $N_S + Q_f$. If additionally $Q_f = 1$, then $V_N^{(i)}$ are all identical for $i = 2, 3, 4$.

2.4. Algebraic formulation. In order to formulate a discrete matrix inequality problem, we introduce matrices and vectors

$$\overline{A}_N(\boldsymbol{\mu}) := (a(\varphi_j, \varphi_i; \boldsymbol{\mu}))_{i,j=1}^{N_V} \in \mathbb{R}^{N_V \times N_V}, \quad \overline{f}_N(\boldsymbol{\mu}) := (f(\varphi_i; \boldsymbol{\mu}))_{i=1}^{N_V} \in \mathbb{R}^{N_V},$$

$$\overline{B}_N := (b(\varphi_i, \xi_j))_{i,j=1}^{N_V, N_W} \in \mathbb{R}^{N_V \times N_W}, \quad \overline{g}_N(\boldsymbol{\mu}) := (g(\xi_i; \boldsymbol{\mu}))_{i=1}^{N_W} \in \mathbb{R}^{N_W}.$$

We then obtain the following algebraic form of $SP_N(\boldsymbol{\mu})$.

LEMMA 2.6 (algebraic reduced basis saddle point problem $DSP_N(\boldsymbol{\mu})$). *The solution $(u_N(\boldsymbol{\mu}), \lambda_N(\boldsymbol{\mu}))$ of the reduced saddle point problem $SP_N(\boldsymbol{\mu})$ expanded as $u_N(\boldsymbol{\mu}) := \sum_{i=1}^{N_V} \overline{u}_{N,i}\varphi_i$ and $\lambda_N(\boldsymbol{\mu}) := \sum_{i=1}^{N_W} \overline{\lambda}_{N,i}\xi_i$, where $\overline{u}_N(\boldsymbol{\mu}) := (\overline{u}_{N,i})_{i=1}^{N_V} \in \mathbb{R}^{N_V}$ and $\overline{\lambda}_N(\boldsymbol{\mu}) := (\overline{\lambda}_{N,i})_{i=1}^{N_W} \in \mathbb{R}^{N_W}$, is equivalently characterized by the matrix inequality system*

$$(2.8) \qquad \overline{A}_N(\boldsymbol{\mu})\overline{u}_N(\boldsymbol{\mu}) + \overline{B}_N\overline{\lambda}_N(\boldsymbol{\mu}) = \overline{f}_N(\boldsymbol{\mu}),$$

$$(2.9) \qquad \overline{\lambda}_N(\boldsymbol{\mu}) \geq 0,$$

$$(2.10) \qquad \overline{g}_N(\boldsymbol{\mu}) - \overline{B}_N^T\overline{u}_N(\boldsymbol{\mu}) \geq 0,$$

$$(2.11) \qquad \overline{\lambda}_N(\boldsymbol{\mu})^T(\overline{g}_N(\boldsymbol{\mu}) - \overline{B}_N^T\overline{u}_N(\boldsymbol{\mu})) = 0.$$

Proof. Equations (2.8)–(2.10) are easy to verify in terms of the definition of the reduced dual cone M_N. By setting $\eta = \lambda_N(\boldsymbol{\mu}) \pm \overline{\lambda}_{N,i}\lambda_N(\boldsymbol{\mu}_i)$, we get the componentwise complementarity condition

$$(2.12) \qquad \overline{\lambda}_{N,i}(\overline{g}_N(\boldsymbol{\mu}) - \overline{B}_N^T\overline{u}_N(\boldsymbol{\mu}))_i = 0, \quad i = 1, \ldots, N_S,$$

where $(\overline{g}_N(\boldsymbol{\mu}) - \overline{B}_N^T\overline{u}_N(\boldsymbol{\mu}))_i$ is the ith coefficient of the vector $\overline{g}_N(\boldsymbol{\mu}) - \overline{B}_N^T\overline{u}_N(\boldsymbol{\mu})$ and thus (2.11). ☐

We point out that $\overline{u}_N(\boldsymbol{\mu})$ is unique, whereas the uniqueness of $\overline{\lambda}_N(\boldsymbol{\mu})$ cannot be guaranteed due to the possible linear dependence of the elements ξ_i. However, all solutions of the coefficient vector $\overline{\lambda}_N(\boldsymbol{\mu})$ represent the same solution function $\lambda_N(\boldsymbol{\mu}) \in M_N$.

2.5. Offline/online decomposition. The parameter dependence of $a(\cdot, \cdot; \boldsymbol{\mu})$, $f(\cdot; \boldsymbol{\mu})$, and $g(\cdot; \boldsymbol{\mu})$ introduced in the previous section transfers into an offline/online decomposition of $DSP_N(\boldsymbol{\mu})$. In the offline-phase, we compute the parameter-independent matrices and vectors $\overline{A}_N^q := (a^q(\varphi_j, \varphi_i))_{i,j=1}^{N_V} \in \mathbb{R}^{N_V \times N_V}$, $\overline{B}_N := (b(\varphi_i, \xi_j))_{i,j=1}^{N_V, N_W} \in \mathbb{R}^{N_V \times N_W}$, $\overline{f}_N^q := (f^q(\varphi_i))_{i=1}^{N_V} \in \mathbb{R}^{N_V}$, $\overline{g}_N^q := (g^q(\xi_i))_{i=1}^{N_W} \in \mathbb{R}^{N_W}$ for q ranging between 1 and Q_a, Q_g, Q_f, respectively. In the online-phase we assemble the parameter-dependent matrices and right-hand sides

$$\overline{A}_N(\boldsymbol{\mu}) = \sum_{q=1}^{Q_a} \theta_a^q(\boldsymbol{\mu})\overline{A}_N^q, \qquad \overline{f}_N(\boldsymbol{\mu}) = \sum_{q=1}^{Q_f} \theta_f^q(\boldsymbol{\mu})\overline{f}_N^q, \qquad \overline{g}_N(\boldsymbol{\mu}) = \sum_{q=1}^{Q_g} \theta_g^q(\boldsymbol{\mu})\overline{g}_N^q$$

and solve the discrete reduced problem $DSP_N(\boldsymbol{\mu})$. The advantage of the method appears in the case $H_W, H_V \gg N_V, N_W$: As all matrices and vectors involved in the online-phase are low-dimensional, the reduced online-phase will be considerably faster than the high-dimensional problem solution.

3. Theoretical results. In this section, we comment on some analytical aspects, namely a consistency result, stability, and Lipschitz-continuity. For all subsequent analytical statements, we assume that V_N and W_N are chosen such that $b(\cdot, \cdot)$ is inf-sup stable on $V_N \times W_N$. Some sufficient conditions on this have been given in Proposition 2.4.

3.1. Reproduction of solutions. Here we state a consistency result which shows that detailed solutions are recovered by the reduced scheme if the corresponding snapshots are contained in the reduced spaces. This could also be formulated as a corollary of the a posteriori error analysis of section 4, but a direct proof is more elegant and elementary.

PROPOSITION 3.1 (reproduction of solutions). *If for some* $\boldsymbol{\mu} \in \mathcal{P}$ *we have* $u(\boldsymbol{\mu}) \in V_N$ *and* $\lambda(\boldsymbol{\mu}) \in M_N$, *then* $u_N(\boldsymbol{\mu}) = u(\boldsymbol{\mu})$ *and* $\lambda_N(\boldsymbol{\mu}) = \lambda(\boldsymbol{\mu})$.

Proof. For $v_N \in V_N$ we directly obtain

$$a(u(\boldsymbol{\mu}), v_N; \boldsymbol{\mu}) + b(v_N, \lambda(\boldsymbol{\mu})) = f(v_N; \boldsymbol{\mu})$$

as $V_N \subset V$ and $(u(\boldsymbol{\mu}), \lambda(\boldsymbol{\mu}))$ solves $SP(\boldsymbol{\mu})$. Similarly, for $\eta_N \in M_N$ we directly obtain

$$b(u(\boldsymbol{\mu}), \eta_N - \lambda(\boldsymbol{\mu})) \le g(\eta_N - \lambda(\boldsymbol{\mu}); \boldsymbol{\mu})$$

as $M_N \subset M$ and $(u(\boldsymbol{\mu}), \lambda(\boldsymbol{\mu}))$ solves $SP(\boldsymbol{\mu})$. Consequently, $(u(\boldsymbol{\mu}), \lambda(\boldsymbol{\mu}))$ solves $SP_N(\boldsymbol{\mu})$. Due to the uniqueness from Proposition 2.4, we conclude that $(u(\boldsymbol{\mu}), \lambda(\boldsymbol{\mu})) = (u_N(\boldsymbol{\mu}), \lambda_N(\boldsymbol{\mu}))$. □

3.2. Boundedness. Next, we show that the solutions are bounded by the data functions of the saddle point problem. Note that, as is typical in RB methods, the analogous result holds for the detailed solution by exchanging the constants. The following a priori result is similar to that for standard variational inequality problems [9]. The continuity and a posteriori analysis of the RB method depends on those, and therefore we recall the details.

PROPOSITION 3.2 (a priori stability estimates). *Let* (V_N, W_N) *be an inf-sup stable pairing. Then, the solution* $(u_N(\boldsymbol{\mu}), \lambda_N(\boldsymbol{\mu}))$ *of* $SP_N(\boldsymbol{\mu})$ *is uniformly bounded with respect to* $\boldsymbol{\mu}$:

$$(3.1) \quad \|u_N(\boldsymbol{\mu})\|_V \le \frac{1}{2\bar{\alpha}} \left(\bar{\gamma}_f + \frac{\bar{\gamma}_a}{\beta_N} \bar{\gamma}_g \right) + \sqrt{\frac{1}{4\bar{\alpha}^2} \left(\bar{\gamma}_f + \frac{\bar{\gamma}_a}{\beta_N} \bar{\gamma}_g \right)^2 + \frac{\bar{\gamma}_g \bar{\gamma}_f}{\bar{\alpha}\beta_N}} =: \bar{\gamma}_u,$$

$$(3.2) \quad \|\lambda_N(\boldsymbol{\mu})\|_W \le \frac{1}{\beta_N} \left(\bar{\gamma}_f + \bar{\gamma}_a \bar{\gamma}_u \right) =: \bar{\gamma}_\lambda.$$

Proof. We start with the proof of (3.2). As $b(\cdot, \cdot)$ is inf-sup stable on $V_N \times W_N$ and V_N is finite-dimensional, there exists a $v_{\lambda_N} \in V_N$ such that

$$\beta_N \|v_{\lambda_N}\|_V \|\lambda_N\|_W \le b(v_{\lambda_N}, \lambda_N) = f(v_{\lambda_N}) - a(u_N, v_{\lambda_N})$$
$$\le \bar{\gamma}_f \|v_{\lambda_N}\|_V + \bar{\gamma}_a \|u_N\|_V \|v_{\lambda_N}\|_V,$$

where the last inequality follows from the uniform continuity of $f(\cdot; \boldsymbol{\mu})$ and $a(\cdot, \cdot; \boldsymbol{\mu})$. Hence

$$(3.3) \qquad\qquad \|\lambda_N\|_W \le \frac{1}{\beta_N} \left(\bar{\gamma}_f + \bar{\gamma}_a \|u_N\|_V \right)$$

and (3.2) follows as soon as (3.1) is established. The complementarity (2.1) also holds for the reduced solution, i.e., $b(u_N, \lambda_N) = g(\lambda_N)$. In terms of coercivity and continuity, we get

$$\bar{\alpha} \|u_N\|_V^2 \leq a(u_N, u_N) = f(u_N) - b(u_N, \lambda_N)$$
$$= f(u_N) - g(\lambda_N) \leq \bar{\gamma}_f \|u_N\|_V + \bar{\gamma}_g \|\lambda_N\|_W .$$

Inserting (3.3) and rearranging the terms, we conclude with

$$\|u_N\|_V^2 - \underbrace{\frac{1}{\bar{\alpha}} \left(\bar{\gamma}_f + \frac{\bar{\gamma}_g \bar{\gamma}_a}{\beta_N} \right)}_{=:p} \|u_N\|_V - \underbrace{\frac{\bar{\gamma}_g \bar{\gamma}_f}{\bar{\alpha} \beta_N}}_{=:q} \leq 0.$$

We observe that $p, q \geq 0$, the quadratic equation $x^2 - px - q = 0$ has real roots $x_1 \leq x_2$, and $\|u_N\|_V \in [x_1, x_2]$ such that we finally obtain (3.1):

$$\|u_N\|_V \leq x_2 = \frac{p}{2} + \sqrt{\frac{p^2}{4} + q} = \bar{\gamma}_u. \quad \square$$

3.3. Lipschitz-continuity. In this section, we are interested in some regularity results of the solutions with respect to the parameter. As we will show, Lipschitz-continuity of the reduced solutions holds under the assumption of Lipschitz-continuity of the data with respect to $\boldsymbol{\mu}$. This result represents an extension of the Lipschitz statement for the linear elliptic case [7] to our nonlinear saddle point problem.

PROPOSITION 3.3 (Lipschitz-continuity with respect to $\boldsymbol{\mu}$). *Let (V_N, W_N) be an inf-sup stable pairing. Then, the solution $(u_N(\boldsymbol{\mu}), \lambda_N(\boldsymbol{\mu}))$ of $SP_N(\boldsymbol{\mu})$ is Lipschitz-continuous with respect to $\boldsymbol{\mu}$, i.e., for all $\boldsymbol{\mu}, \boldsymbol{\mu}'$ it holds that*

$$(3.4) \qquad \|u_N(\boldsymbol{\mu}) - u_N(\boldsymbol{\mu}')\|_V \leq L_u \|\boldsymbol{\mu} - \boldsymbol{\mu}'\|,$$

$$(3.5) \qquad \|\lambda_N(\boldsymbol{\mu}) - \lambda_N(\boldsymbol{\mu}')\|_W \leq L_\lambda \|\boldsymbol{\mu} - \boldsymbol{\mu}'\|,$$

with constants independent of $\boldsymbol{\mu}, \boldsymbol{\mu}'$:

$$L_u := C_1 + \sqrt{C_1^2 + C_2}, \qquad L_\lambda := \frac{1}{\beta_N} \left(L_f + L_a \bar{\gamma}_u + \bar{\gamma}_a L_u \right),$$

$$C_1 := \frac{1}{2\bar{\alpha}} \left(\frac{L_g \bar{\gamma}_a}{\beta_N} + L_f + L_a \bar{\gamma}_u \right), \qquad C_2 := \frac{L_g}{\bar{\alpha} \beta_N} \left(L_f + L_a \bar{\gamma}_u \right).$$

Here $L_a, L_f,$ and L_g are the Lipschitz-constants of $a(\cdot, \cdot; \boldsymbol{\mu}), f(\cdot; \boldsymbol{\mu}),$ and $g(\cdot; \boldsymbol{\mu}),$ and $\bar{\gamma}_u$ is defined by (3.1).

Proof. We assume $\boldsymbol{\mu}, \boldsymbol{\mu}' \in \mathcal{P}$ and introduce some abbreviations (with slight abuse of notation) to facilitate the readability: $u := u_N(\boldsymbol{\mu}), u' := u_N(\boldsymbol{\mu}'), \lambda := \lambda_N(\boldsymbol{\mu}), \lambda' := \lambda_N(\boldsymbol{\mu}'), a(\cdot, \cdot) := a(\cdot, \cdot; \boldsymbol{\mu}), a'(\cdot, \cdot) := a(\cdot, \cdot; \boldsymbol{\mu}'), f(\cdot) := f(\cdot; \boldsymbol{\mu}), f'(\cdot) := f(\cdot; \boldsymbol{\mu}'), g(\cdot) := g(\cdot; \boldsymbol{\mu}), g'(\cdot) := g(\cdot; \boldsymbol{\mu}').$ Then, obviously we have

$$(3.6) \qquad a(u, v) + b(v, \lambda) = f(v), \quad v \in V_N,$$

$$(3.7) \qquad a'(u', v) + b(v, \lambda') = f'(v), \quad v \in V_N.$$

Due to the inf-sup stability for $\lambda - \lambda' \in W_N$ there exists a $v \in V_N$ with

$$\beta_N \|v\|_V \|\lambda - \lambda'\|_W \leq b(v, \lambda - \lambda') = b(v, \lambda) - b(v, \lambda')$$
$$= f(v) - a(u, v) - f'(v) + a'(u', v) + a(u', v) - a(u', v)$$
$$\leq L_f \|v\|_V \|\boldsymbol{\mu} - \boldsymbol{\mu}'\| + L_a \|u'\|_V \|v\|_V \|\boldsymbol{\mu} - \boldsymbol{\mu}'\| + \bar{\gamma}_a \|u - u'\|_V \|v\|_V .$$

Using the boundedness of u' due to Proposition 3.2, we obtain

$$(3.8) \qquad \|\lambda - \lambda'\|_W \le \frac{1}{\beta_N} \left((L_f + L_a \bar{\gamma}_u) \|\boldsymbol{\mu} - \boldsymbol{\mu}'\| + \bar{\gamma}_a \|u - u'\|_V \right).$$

Now, the inequality of the saddle point problem yields

$$\begin{aligned} b(u - u', \lambda' - \lambda) &= b(u, \lambda' - \lambda) + b(u', \lambda - \lambda') \\ &\le g(\lambda' - \lambda) + g'(\lambda - \lambda') \le L_g \|\lambda' - \lambda\|_W \|\boldsymbol{\mu} - \boldsymbol{\mu}'\|. \end{aligned}$$

Moreover, we find for $v \in V_N$ that

$$\begin{aligned} a(u - u', v) &= a(u, v) - a(u', v) \\ &= -b(v, \lambda) + f(v) - a(u', v) + a'(u', v) + b(v, \lambda') - f'(v) \\ &\le b(v, \lambda' - \lambda) + L_f \|v\|_V \|\boldsymbol{\mu} - \boldsymbol{\mu}'\| + L_a \|u'\|_V \|v\|_V \|\boldsymbol{\mu} - \boldsymbol{\mu}'\|. \end{aligned}$$

Then, the coercivity in combination with $v = u - u'$ guarantees

$$\begin{aligned} \bar{\alpha} \|u - u'\|_V^2 &\le a(u - u', u - u') \\ &\le L_g \|\lambda' - \lambda\|_W \|\boldsymbol{\mu} - \boldsymbol{\mu}'\| \\ &\quad + L_f \|u - u'\|_V \|\boldsymbol{\mu} - \boldsymbol{\mu}'\| + L_a \|u'\|_V \|u - u'\|_V \|\boldsymbol{\mu} - \boldsymbol{\mu}'\|. \end{aligned}$$

Using the boundedness of u', this simplifies to

$$\|u - u'\|_V^2 \le \frac{1}{\bar{\alpha}} \|\boldsymbol{\mu} - \boldsymbol{\mu}'\| \left(L_g \|\lambda' - \lambda\|_W + (L_f + L_a \bar{\gamma}_u) \|u - u'\|_V \right).$$

Inserting (3.8) and rearranging the terms gives

$$\begin{aligned} \|u - u'\|_V^2 &- \frac{1}{\bar{\alpha}} \left(\frac{L_g \bar{\gamma}_a}{\beta_N} + L_f + L_a \bar{\gamma}_u \right) \|\boldsymbol{\mu} - \boldsymbol{\mu}'\| \, \|u - u'\|_V \\ &- \left(\frac{L_g}{\bar{\alpha} \beta_N} (L_f + L_a \bar{\gamma}_u) \right) \|\boldsymbol{\mu} - \boldsymbol{\mu}'\|^2 \le 0. \end{aligned}$$

We argue as in the proof of Proposition 3.2: Using that the left-hand side is of the form $x^2 - 2C_1 \|\boldsymbol{\mu} - \boldsymbol{\mu}'\| x - C_2 \|\boldsymbol{\mu} - \boldsymbol{\mu}'\|^2$ and has real roots $x_1 \le x_2$, we conclude that $\|u - u'\|_V < x_2$, which proves (3.4). Inserting the last result in (3.8) finally gives (3.5).   □

4. A posteriori error analysis. In this section, we focus on the efficient control of the reduction error by a posteriori error estimators. Adaptive techniques based on a posteriori error estimators play an important role in enhancing the performance of finite element discretizations. For abstract variational inequalities in the context of finite elements, we refer the reader to [1, 4] and note that, in general, the lower bound is problematic. Also in RB methods, a posteriori error bounds can be applied in adaptive basis enrichment schemes, such as the greedy algorithm [3, 6, 7, 11, 24].

4.1. Preliminaries. We start by introducing suitable functionals which characterize the error of the reduced solution. First, we define the equality residual $r(\cdot; \boldsymbol{\mu}) \in V'$ by

$$(4.1) \qquad r(v; \boldsymbol{\mu}) := f(v; \boldsymbol{\mu}) - a(u_N(\boldsymbol{\mu}), v; \boldsymbol{\mu}) - b(v, \lambda_N(\boldsymbol{\mu})), \quad v \in V.$$

Next, we quantify the inequality error by an inequality residual $s(\cdot; \boldsymbol{\mu}) \in W'$ with

$$(4.2) \qquad s(\eta; \boldsymbol{\mu}) := b(u_N(\boldsymbol{\mu}), \eta) - g(\eta; \boldsymbol{\mu}), \quad \eta \in W.$$

The residual $r(\cdot; \boldsymbol{\mu})$ represents the right-hand side of the error-equation, i.e.,

$$(4.3) \qquad a(u(\boldsymbol{\mu}) - u_N(\boldsymbol{\mu}), v; \boldsymbol{\mu}) + b(v, \lambda(\boldsymbol{\mu}) - \lambda_N(\boldsymbol{\mu})) = r(v; \boldsymbol{\mu}), \quad v \in V.$$

Equality and inequality residuals can be quantified on V_N and M_N by

$$(4.4) \qquad r(v_N; \boldsymbol{\mu}) = 0, \quad v_N \in V_N, \qquad s(\eta_N; \boldsymbol{\mu}) \le 0, \quad \eta_N \in M_N.$$

Moreover, we point out that for the special case of $u_N(\boldsymbol{\mu}) = u(\boldsymbol{\mu})$ and $\lambda_N(\boldsymbol{\mu}) = \lambda(\boldsymbol{\mu})$ we have $r(v; \boldsymbol{\mu}) = 0$ and $s(\eta; \boldsymbol{\mu}) \le 0$ for all $v \in V, \eta \in M$. Hence, the deviation from this equality/inequality gives information about the error and needs to be controlled. In order to quantify the error, we first introduce the Riesz-representers $v_r(\boldsymbol{\mu}) \in V, \eta_s(\boldsymbol{\mu}) \in W$ of the residuals

$$\langle v, v_r(\boldsymbol{\mu}) \rangle_V = r(v; \boldsymbol{\mu}), \quad v \in V, \qquad \langle \eta, \eta_s(\boldsymbol{\mu}) \rangle_W = s(\eta; \boldsymbol{\mu}), \quad \eta \in W.$$

Additionally, we denote $\tilde{\eta}_s(\boldsymbol{\mu}) \in W$ to be the Riesz-representer of the detailed inequality functional defined by

$$(4.5) \qquad \langle \tilde{\eta}_s(\boldsymbol{\mu}), \eta \rangle_W = b(u(\boldsymbol{\mu}), \eta) - g(\eta; \boldsymbol{\mu}), \quad \eta \in W.$$

These ingredients also are required for RB error estimation for the Stokes problem [19]. We point out a major difference to this procedure: The incompressibility condition is an equality constraint, and its violation can be measured by a pressure residual (corresponding to our $s(\cdot; \boldsymbol{\mu})$). Therefore, $\|s\|_{W'}$ is a straightforward error estimator component. In our case we cannot do this due to the inequality. We obviously would correctly penalize if $s(\eta; \boldsymbol{\mu}) > 0$ for some $\eta \in M$ as desired, but we would also penalize $s(\eta; \boldsymbol{\mu}) < 0$, which is not necessary. Hence, we need to cope with the inherent nonlinearity induced by the inequalities. For this, we require a projection $\pi : W \to M$ which we assume to be an orthogonal projection with respect to a scalar-product $\langle \cdot, \cdot \rangle_\pi$ on W endowed with the induced norm $\|\eta\|_\pi := \sqrt{\langle \eta, \eta \rangle_\pi}$ being equivalent to the W-norm via $c_\pi \|\eta\|_W \le \|\eta\|_\pi \le C_\pi \|\eta\|_W$ for suitable constants $0 < c_\pi \le C_\pi$. Moreover, we assume that π satisfies the following properties:

$$(4.6) \qquad \langle \eta - \pi(\eta), \eta' \rangle_W \le 0, \quad \eta \in W, \ \eta' \in M,$$
$$(4.7) \qquad \pi(\tilde{\eta}_s) = 0,$$
$$(4.8) \qquad \langle \eta, \tilde{\eta}_s \rangle_\pi \le 0, \quad \eta \in M.$$

For example, these conditions are met by standard orthogonal projections with $\langle \cdot, \cdot \rangle_\pi = \langle \cdot, \cdot \rangle_W$. Other problem specific choices will be given in section 5. However, note that such a projection operator will in general be nonlinear. We state a connection between the primal and dual error, which will be used for the a posteriori error estimators.

LEMMA 4.1 (primal/dual error relation). *For any* $\boldsymbol{\mu} \in \mathcal{P}$ *the dual error can be bounded by the primal error as*

$$(4.9) \qquad \|\lambda(\boldsymbol{\mu}) - \lambda_N(\boldsymbol{\mu})\|_W \le \frac{1}{\beta} \left(\|r(\cdot; \boldsymbol{\mu})\|_{V'} + \gamma_a(\boldsymbol{\mu}) \|u(\boldsymbol{\mu}) - u_N(\boldsymbol{\mu})\|_V \right).$$

Proof. The inf-sup stability of $b(\cdot, \cdot)$ guarantees the existence of an $v \in V$, $v \neq 0$, such that with (4.3)

$$\beta \|v\|_V \|\lambda - \lambda_N\|_W \leq b(v, \lambda - \lambda_N) = r(v) + a(u_N - u, v)$$
$$\leq \|v\|_V \|r\|_{V'} + \gamma_a \|v\|_V \|u - u_N\|_V,$$

and the result follows. □

4.2. A posteriori error estimators. We can now present a posteriori error bounds.

PROPOSITION 4.2 (upper a posteriori error bound). *For any $\boldsymbol{\mu}$ we define the residual estimators*

$$(4.10) \qquad \delta_r(\boldsymbol{\mu}) := \|r(\cdot; \boldsymbol{\mu})\|_{V'} = \|v_r(\boldsymbol{\mu})\|_V,$$

$$(4.11) \qquad \delta_{s1}(\boldsymbol{\mu}) := \|\pi(\eta_s(\boldsymbol{\mu}))\|_W,$$

$$(4.12) \qquad \delta_{s2}(\boldsymbol{\mu}) := \langle \lambda_N(\boldsymbol{\mu}), \pi(\eta_s(\boldsymbol{\mu})) \rangle_W.$$

Then, the RB errors can be bounded by

$$(4.13) \qquad \|u(\boldsymbol{\mu}) - u_N(\boldsymbol{\mu})\|_V \leq \Delta_u(\boldsymbol{\mu}) := c_1(\boldsymbol{\mu}) + \sqrt{c_1(\boldsymbol{\mu})^2 + c_2(\boldsymbol{\mu})},$$

$$(4.14) \qquad \|\lambda(\boldsymbol{\mu}) - \lambda_N(\boldsymbol{\mu})\|_W \leq \Delta_\lambda(\boldsymbol{\mu}) := \frac{1}{\beta} \left(\delta_r(\boldsymbol{\mu}) + \gamma_a(\boldsymbol{\mu}) \Delta_u(\boldsymbol{\mu}) \right),$$

with constants

$$c_1(\boldsymbol{\mu}) := \frac{1}{2\alpha(\boldsymbol{\mu})} \left(\delta_r(\boldsymbol{\mu}) + \frac{\delta_{s1}(\boldsymbol{\mu}) \gamma_a(\boldsymbol{\mu})}{\beta} \right), \quad c_2(\boldsymbol{\mu}) := \frac{1}{\alpha(\boldsymbol{\mu})} \left(\frac{\delta_{s1}(\boldsymbol{\mu}) \delta_r(\boldsymbol{\mu})}{\beta} + \delta_{s2}(\boldsymbol{\mu}) \right).$$

Proof. We note that (4.14) is a direct consequence of (4.13) and (4.9). Hence, it remains to show (4.13). Using coercivity, the error-equation (4.3), $b(u, \lambda_N - \lambda) \leq g(\lambda_N - \lambda)$, the definitions of the residuals, and $\langle \lambda, \eta_s - \pi(\eta_s) \rangle_W \leq 0$ leads to

$$\alpha \|u - u_N\|_V^2 \leq a(u - u_N, u - u_N) = r(u - u_N) - b(u - u_N, \lambda - \lambda_N)$$
$$\leq \delta_r \|u - u_N\|_V + b(u, \lambda_N - \lambda) + b(u_N, \lambda - \lambda_N)$$
$$\leq \delta_r \|u - u_N\|_V + g(\lambda_N - \lambda) + s(\lambda - \lambda_N) + g(\lambda - \lambda_N)$$
$$= \delta_r \|u - u_N\|_V + \langle \lambda, \pi(\eta_s) \rangle_W + \langle \lambda, \eta_s - \pi(\eta_s) \rangle_W$$
$$\leq \delta_r \|u - u_N\|_V + \langle \lambda - \lambda_N, \pi(\eta_s) \rangle_W + \delta_{s2}$$
$$\leq \delta_r \|u - u_N\|_V + \|\lambda - \lambda_N\|_W \delta_{s1} + \delta_{s2}.$$

Inserting (4.9) yields

$$\|u - u_N\|_V^2 - \frac{1}{\alpha} \left(\delta_r + \frac{\delta_{s1} \gamma_a}{\beta} \right) \|u - u_N\|_V - \frac{1}{\alpha} \left(\frac{\delta_{s1} \delta_r}{\beta} + \delta_{s2} \right) \leq 0.$$

Using the same argumentation as in previous proofs, i.e., bounding the error by the largest root of the corresponding quadratic polynomial, gives the bound (4.13). □

We briefly comment on the different terms in the upper bound. In the ideal case of $u_N(\boldsymbol{\mu}) = u(\boldsymbol{\mu})$, $\lambda_N(\boldsymbol{\mu}) = \lambda(\boldsymbol{\mu})$ we obtain $\delta_r(\boldsymbol{\mu}) = \delta_{s1}(\boldsymbol{\mu}) = \delta_{s2}(\boldsymbol{\mu}) = 0$ by (4.7). Then, the error bounds also yield $\Delta_u(\boldsymbol{\mu}) = \Delta_\lambda(\boldsymbol{\mu}) = 0$, identifying exact approximation a posteriori, i.e., in the online-phase.

Let us assume an unconstrained case of $\lambda_N(\boldsymbol{\mu}) = 0$ and $b(u_N(\boldsymbol{\mu}), \eta) \leq g(\eta; \boldsymbol{\mu})$ for all $\eta \in M$. Then, it is easy to see that $\delta_{s1}(\boldsymbol{\mu}) = \delta_{s2}(\boldsymbol{\mu}) = 0$, and we perfectly reproduce the tight a posteriori bound for the elliptic equations of [22]: $\Delta_u(\boldsymbol{\mu}) = \frac{\|r\|_{V'}}{\alpha(\boldsymbol{\mu})}$.

An interesting fact is that the equality residual can be observed to vanish in certain situations.

PROPOSITION 4.3 (vanishing equality residual). *Let $Q_a = 1$, and let the reduced primal space V_N be chosen as (2.6). Then, we obtain $r(\cdot; \boldsymbol{\mu}) = 0$.*

Proof. Again, w.l.o.g., let $a(\cdot, \cdot)$ be nonparametric; then the definition of the equality residual and of the operators A and C yield

$$r(v; \boldsymbol{\mu}) = \sum_{q=1}^{Q_f} \theta_f^q(\boldsymbol{\mu}) a(A f^q, v) - a(u_N(\boldsymbol{\mu}), v) - a(C\lambda_N(\boldsymbol{\mu}), v) = a(z, v),$$

with $z := \sum_{q=1}^{Q_f} \theta_f^q(\boldsymbol{\mu}) A f^q - u_N(\boldsymbol{\mu}) - C\lambda_N(\boldsymbol{\mu}) \in V_N$. As $r(\cdot; \boldsymbol{\mu})$ vanishes on V_N, we obtain

$$0 = r(z; \boldsymbol{\mu}) = a(z, z) \geq \alpha \|z\|^2.$$

Therefore, $z = 0$, and consequently $r(v) = a(0, v) = 0$, $v \in V$. $\square$

The residuals not only provide an upper bound for the error in Proposition 4.2 but also yield lower bounds.

PROPOSITION 4.4 (lower a posteriori error bounds). *For any $\boldsymbol{\mu} \in \mathcal{P}$ the following lower bounds for the reduction error hold:*

$$(4.15) \qquad \delta_r(\boldsymbol{\mu}) \leq \gamma_a(\boldsymbol{\mu}) \|u(\boldsymbol{\mu}) - u_N(\boldsymbol{\mu})\|_V + \gamma_b \|\lambda(\boldsymbol{\mu}) - \lambda_N(\boldsymbol{\mu})\|_W,$$

$$(4.16) \qquad \delta_{s1}(\boldsymbol{\mu}) \leq \frac{\gamma_b C_\pi}{c_\pi} \|u(\boldsymbol{\mu}) - u_N(\boldsymbol{\mu})\|_V,$$

$$(4.17) \qquad \delta_{s2}(\boldsymbol{\mu}) \leq \frac{\bar{\gamma}_\lambda \gamma_b C_\pi}{c_\pi} \|u(\boldsymbol{\mu}) - u_N(\boldsymbol{\mu})\|_V.$$

Proof. Thanks to the error-equation (4.3), we obtain with the Riesz-representation $v_r \in V$ of $r \in V'$

$$\gamma_a(\boldsymbol{\mu}) \|u - u_N\|_V \|v_r\|_V + \gamma_b \|\lambda - \lambda_N\|_W \|v_r\|_V \geq a(u - u_N, v_r) + b(v_r, \lambda - \lambda_N)$$
$$= r(v_r) = \langle v_r, v_r \rangle_V = \|v_r\|_V^2,$$

which gives (4.15).

We note that orthogonal projections on convex sets have Lipschitz-constant one. Thus (4.7) and the norm-equivalence on V guarantee

$$\delta_{s1} = \|\pi(\eta_s) - \pi(\tilde{\eta}_s)\|_W \leq \frac{1}{c_\pi} \|\pi(\eta_s) - \pi(\tilde{\eta}_s)\|_\pi \leq \frac{1}{c_\pi} \|\eta_s - \tilde{\eta}_s\|_\pi \leq \frac{C_\pi}{c_\pi} \|\eta_s - \tilde{\eta}_s\|_W.$$

For the last term we continue with

$$\|\eta_s - \tilde{\eta}_s\|_W = \sup_{\eta \in W} \frac{b(u_N, \eta) - g(\eta) - b(u, \eta) + g(\eta)}{\|\eta\|_W} = \sup_{\eta \in W} \frac{b(u_N - u, \eta)}{\|\eta\|_W}$$

$$(4.18) \qquad \leq \sup_{\eta \in W} \frac{\gamma_b \|u_N - u\|_V \|\eta\|_W}{\|\eta\|_W} \leq \gamma_b \|u_N - u\|_V,$$

from which we can conclude (4.16).

The lower bound (4.17) follows from (4.16) and the observation that $\delta_{s2} \leq \bar{\gamma}_\lambda \|\pi(\eta_s)\|_W$. $\quad\square$

Remark 4.5. A closer look at the lower and upper bounds given in Propositions 4.4 and 4.2 reveals a gap. In the upper bound the term $\sqrt{\delta_{s2}}$ enters, whereas in the lower bound the term δ_{s2} appears. This results from the variational inequality setting.

Remark 4.6. We point out that the lower bounds strongly depend on the constants c_π and C_π. If we choose $\langle \cdot, \cdot \rangle_\pi := \langle \cdot, \cdot \rangle_W$, these are independent of the discretization $C_\pi = c_\pi = 1$, but then the evaluation of π has the same complexity as the original problem. To reduce the computational cost, alternative scalar products can be selected, but then C_π/c_π possibly depends on the high dimension H_W and is possibly quite large. In that case, the lower bounds are not very informative.

We close this section with a short comment on the decomposition of $\Delta_u(\boldsymbol{\mu}), \Delta_\lambda(\boldsymbol{\mu})$. In contrast to a posteriori estimators in many other RB methods, these are currently not fully decomposable in an offline/online fashion due to the nonlinear projection. To be precise, the δ_r can be fully decomposed similarly as for standard RB problems. But for computation of the more relevant quantities δ_{s1}, δ_{s2} we cannot avoid computing the high-dimensional projection π. Still, the evaluation of the error estimators is much cheaper than solving the detailed problem, as will be demonstrated in the experiments.

5. Implementational aspects. In this section, we comment on computational aspects that are required for the realization of the reduced scheme and our experiments. Quite often W is the dual space of a finite-dimensional V which simplifies some computations, as the dimensions coincide, and the inner products are related.

5.1. Solution of the detailed and reduced problem. In practice it is quite common to choose the basis of W such that the matrix associated with $b(\cdot, \cdot)$ has a simple diagonal form; this property is often referred to as biorthogonality. This makes the use of a primal-dual active set strategy for the high-dimensional problem associated with the snapshots computationally attractive; cf. [13, 15].

For the reduced problem (2.8)–(2.11), different solvers such as interior point methods, SQP, and penalty techniques can be applied. Here, we do not require a special biorthogonalization of the basis of V_N with respect to the vectors spanning M_N. Hence, we accept that the matrix $\overline{B}_N$ is now possibly dense. It is easy to show that the solution of $DSP_N(\boldsymbol{\mu})$ is equivalent to the solution of a constrained convex quadratic optimization problem; cf. the variational minimization problem (1.1).

Remark 5.1 (discrete quadratic program $DQP_N(\boldsymbol{\mu})$). The solution vectors $(\overline{u}_N(\boldsymbol{\mu}), \overline{\lambda}_N(\boldsymbol{\mu}))$ of $DSP_N(\boldsymbol{\mu})$ are equivalently obtained as solution of a constrained convex quadratic optimization problem. In particular, $\overline{u}_N(\boldsymbol{\mu})$ is the unique minimizer of

$$(5.1) \qquad \min \frac{1}{2} \overline{v}_N^T \overline{A}_N(\boldsymbol{\mu}) \overline{v}_N - \overline{f}_N(\boldsymbol{\mu})^T \overline{v}_N$$

$$(5.2) \qquad \text{s.t.} \qquad \overline{B}_N^T \overline{v}_N \leq \overline{g}_N(\boldsymbol{\mu}),$$

and $\overline{\lambda}_N(\boldsymbol{\mu})$ is a nonnegative vector of Lagrange multipliers in the optimum, i.e., $\overline{A}_N \overline{u}_N + \overline{B}_N \overline{\lambda}_N = \overline{f}_N$ and $\overline{\lambda}_{N,i} = 0$ if $(\overline{B}_N^T \overline{u}_N - \overline{g}_N)_i < 0$.

Hence, any off-the-shelf quadratic optimization routine using Lagrange multipliers can be used to compute $\overline{u}_N(\boldsymbol{\mu})$ and $\overline{\lambda}_N(\boldsymbol{\mu})$. Note that we did not assume linear independence of the dual snapshots in the construction of the reduced cone. Therefore,

the inequality system may have linearly dependent rows. As mentioned above, this may lead to a nonunique vector $\overline{\lambda}_N$ but a unique function $\lambda_N(\boldsymbol{\mu})$.

5.2. Choice of the projection for the case $W = V'$. For the special case of $W = V'$, we could use the $\langle \cdot, \cdot \rangle_W$ inner product and the corresponding orthogonal projection for the error estimators. Here, for computational simplicity we use a different projection. First, we make some further assumptions on the problem. We suppose that W is endowed with a basis $\{\chi_i\}_i$ such that M can be written as $M = \mathrm{span}_+\{\chi_i\}_{i=1}^{H_W}$. For obstacle-type problems this is natural to hold in the finite element setting, since $\{\chi_i\}_{i=1}^{H_W}$ can be chosen as a dual basis of $\{\psi_i\}_{i=1}^{H_V}$. We then have $H_V = H_W =: H$ with the inner product matrices $\underline{M}^V := (\langle \psi_i, \psi_j \rangle_V)_{i,j=1}^H$ and $\underline{M}^W := (\langle \chi_i, \chi_j \rangle_W)_{i,j=1}^H$. These matrices allow us to compute inner products and norms as required in the a posteriori error bounds. For instance, for any $\eta, \eta' \in W$ with coefficient vectors $\underline{\eta}, \underline{\eta}' \in \mathbb{R}^H$ we have $\langle \eta, \eta' \rangle_W = \underline{\eta}^T \underline{M}^W \underline{\eta}'$. In the case of $W = V'$ one can even verify that $\underline{M}^W = (\underline{M}^V)^{-1}$. If $\underline{M}^V$ is an M-matrix, which is typical for finite element discretization spaces, one can even guarantee that $\underline{M}^W$ has nonnegative entries. We define $\pi : W \to M$ as follows:

$$(5.3) \qquad \pi(\eta) = \sum_{i=1}^H \underline{\pi}_i \chi_i, \quad \underline{\pi} = (\underline{\pi}_i)_{i=1}^H := (\underline{M}^W)^{-1}[\underline{M}^W \underline{\eta}]_+,$$

with $[\cdot]_+$ denoting the componentwise positive part of a vector. An element $\eta \in W$ is in M if and only if $\underline{\eta}_i \geq 0$ for all indices i. Hence, with $\underline{M}^V$ being an M-matrix, we obtain $\underline{M}^W \underline{\eta} \geq 0$ for $\underline{\eta} \geq 0$. Thus for $\eta \in M$, we have $[\underline{M}^W \underline{\eta}]_+ = \underline{M}^W \underline{\eta}$ and $\pi(\eta) = \eta$. We define an alternative inner product on W by $\langle \eta, \eta' \rangle_\pi := \underline{\eta}^T (\underline{M}^W)^2 \underline{\eta}'$. Symmetry, bilinearity, and positive definiteness are obviously inherited from the inner product of W. One can verify that π from (5.3) is the orthogonal projection on M with respect to $\langle \cdot, \cdot \rangle_\pi$ and that it satisfies the assumptions (4.6)–(4.8). Therefore, π can be applied in the a posteriori error bounds. We note that the dense matrix $\underline{M}^W$ which enters formally in the definition of π is not required to evaluate δ_{s1} and δ_{s2}. By definition (4.11), (4.12), we have

$$\begin{aligned}
\delta_{s1}^2 &= \left((\underline{M}^W)^{-1}[\underline{M}^W \underline{\eta}_s(\boldsymbol{\mu})]_+ \right)^T \underline{M}^W (\underline{M}^W)^{-1}[\underline{M}^W \underline{\eta}_s(\boldsymbol{\mu})]_+ \\
&= [\underline{B}^T \underline{u}_N(\boldsymbol{\mu}) - \underline{g}(\boldsymbol{\mu})]_+^T \underline{M}^V [\underline{B}^T \underline{u}_N(\boldsymbol{\mu}) - \underline{g}(\boldsymbol{\mu})]_+, \\
\delta_{s2} &= \underline{\lambda}_N(\boldsymbol{\mu})^T \underline{M}^W (\underline{M}^W)^{-1}[\underline{M}^W \underline{\eta}_s(\boldsymbol{\mu})]_+ \\
&= \underline{\lambda}_N(\boldsymbol{\mu})^T [\underline{B}^T \underline{u}_N(\boldsymbol{\mu}) - \underline{g}(\boldsymbol{\mu})]_+.
\end{aligned}$$

We observe that this equivalent representation of δ_{s1} and δ_{s2} shows directly that these contributions are equal to zero if the reduced solution $u_N(\boldsymbol{\mu}) \in X(\boldsymbol{\mu})$, and thus these terms can be regarded as a measure for the violation of the constraint.

6. Numerical results. In this section, we test our approach on some obstacle type examples in one dimension. We consider an "elastic" rope hanging over a surface that may cause contact. Our setting is as follows: The domain $\Omega = (0, 1)$ is discretized with a uniform mesh of step size $\Delta x := 1/K$ for $K \in \mathbb{N}$. For the discrete function space V, we use standard conforming nodal first order finite elements $V := \{v \in H_0^1(\Omega)|v_{|[x_k, x_{k+1}]} \in P_1, k = 0, \dots, K - 1\}$ of dimension $H_V = H_W = H := K - 1 = 201$ with $x_k := k\Delta x$. We associate the basis function $\psi_i \in V$ with its Lagrange

node $x_i \in \Omega$, i.e., $\psi_i(x_j) = \delta_{ij}$, $i, j = 1, \ldots, H$. The discretization of the Lagrange multipliers is performed using a dual finite element basis of $W = V'$. The cone M is defined by $M := \mathrm{span}_+\{\chi_i\}_{i=1}^H$.

We want to consider the case $Q_a = 1$ and $Q_a > 1$ separately and illuminate different aspects. For this we introduce the following two models.

Model I, $Q_a = 1$. We choose the parameter domain $\mathcal{P} := [0.001, 0.01] \subset \mathbb{R}$. The parameter vector is a scalar parameter $\boldsymbol{\mu} = (\mu)$. The bilinear forms a and b are given by

$$a(u, v; \boldsymbol{\mu}) := \int_\Omega \nu(\boldsymbol{\mu})(x) \nabla u(x) \cdot \nabla v(x) dx, \quad u, v \in V,$$
$$b(u, \eta) := -\eta(u), \quad u \in V,\ \eta \in W,$$

with $\nu(\boldsymbol{\mu})(x) = \mu$, which characterizes the "elasticity" of the rope. As we use a dual finite element basis, the matrix $\underline{B} = (b(\psi_i, \chi_j))_{i,j=1}^{H,H}$ corresponding to the bilinear form $b(\cdot, \cdot)$ is a multiple of the identity. The right-hand-side functional f corresponds to gravity and is nonparametric:

$$f(v; \boldsymbol{\mu}) = f(v) := -\int_\Omega v(x) dx, \quad v \in V.$$

The obstacle is given as

$$g(\eta; \boldsymbol{\mu}) = \sum_{i=1}^H \underline{\eta}_i h(x_i; \boldsymbol{\mu}) \quad \text{for} \quad \eta = \sum_{i=1}^H \underline{\eta}_i \chi_i \in W$$

with a parameter-independent barrier function $h(x) = 5x - 10$.

Model II, $Q_a > 1$. To get a more complex example, we modify Model I by increasing the parameter dimension and replacing the barrier and the elasticity function. The parameter domain is now $\mathcal{P} := [0.05, 0.25] \times [-0.05, 0.5] \subset \mathbb{R}^2$, and the parameter vector consists of a pair of parameters $\boldsymbol{\mu} = (\mu_1, \mu_2)$. We choose the elasticity $\nu(\boldsymbol{\mu})(x) = \mu_1 Ind_{[0,1/2]}(x) + \nu_0 Ind_{[1/2,1]}(x)$, where we denote the characteristic function of an interval Γ by Ind_Γ. We use the fixed value $\nu_0 = 0.15$. This gives rise to $Q_a = 2$ components in the bilinear form $a(\cdot, \cdot; \boldsymbol{\mu})$ corresponding to the two subinterval integrals. We choose a parameter-dependent obstacle functional $g(\cdot; \boldsymbol{\mu})$ defined as above using the barrier function

$$h(x; \boldsymbol{\mu}) = -0.2 \left(\sin(\pi x) - \sin(3\pi x) \right) - 0.5 + \mu_2(x - 0.5).$$

We keep the parameter-independent functional $f(\cdot)$ and bilinear form $b(\cdot, \cdot)$ as in Model I.

6.1. Examples of numerical solutions. We want to demonstrate the basic behavior of the RB scheme. In Figure 6.1 (left and middle columns), we present examples of primal and dual RB solutions for Model II while varying the two parameters. Similar visualization results can be obtained for Model I.

In the offline-phase, we compute the snapshots, i.e., a set of detailed solutions of our obstacle problem corresponding to various values $\boldsymbol{\mu}_i$ of the parameter $\boldsymbol{\mu}$. The reduced basis $\{\varphi_i\}_{i=1}^{N_V}$ is taken as an orthonormal family of $V_N = V_N^{(2)}$ given by (2.5). The dual reduced space is chosen as $W_N := W_N^{(1)}$ from (2.2). In our test, we consider
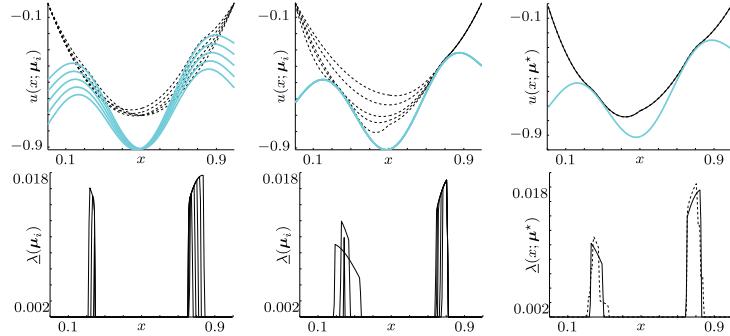
FIG. 6.1. *Examples corresponding to Model* II. *Top: primal solutions and obstacle. Bottom: dual solutions. Left column: the RB parameters are associated with the obstacle with μ_2 values uniformly distributed in $[-0.05, 0.5]$ and constant elasticity $\mu_1 = 0.15$. Middle column: the RB parameters are associated with the elasticity with μ_1 values uniformly distributed in $[0.05, 0.25]$ and a fixed obstacle for $\mu_2 = 0.225$. Right column: exact and reduced solutions for $\boldsymbol{\mu}^* = (0.075, 0.4)^T$. Solid line: exact solutions; dashed line: reduced solutions.*

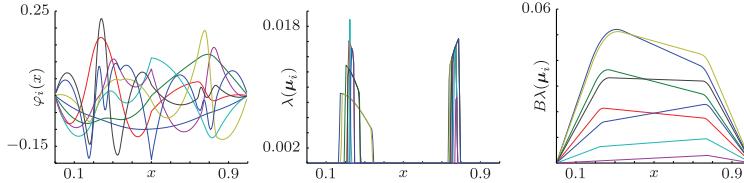

FIG. 6.2. *First eight vectors of the reduced basis $\{\varphi_i\}_{i=1}^{N_V}$ forming V_N (left), of the dual reduced family $\{\lambda(\boldsymbol{\mu}_i)\}_{i=1}^{N_S}$ (middle), and of the corresponding supremizers $\{B\lambda(\boldsymbol{\mu}_i)\}_{i=1}^{N_S}$ (right).*

$N_S = 25$ values of $\boldsymbol{\mu}$ taken on a 5×5 grid composed of uniformly distributed points. Thanks to a standard singular value decomposition routine, we extract from the family $\{u(\boldsymbol{\mu}_i), B\lambda(\boldsymbol{\mu}_i)\}$ an orthonormal basis using the eigenvectors of the corresponding correlation matrix associated with eigenvalues larger than a tolerance $Tol = 10^{-8}$. As a consequence, $N_V = 32$ vectors are considered as reduced basis for the primal variable.

An example of the exact and reduced solutions corresponding to the (nonsnapshot) parameter $\boldsymbol{\mu}^* = (0.075, 0.4)^T$ is depicted in the right column of Figure 6.1. We see that the reduced and exact primal solutions $u_N(\boldsymbol{\mu}^*)$ and $u(\boldsymbol{\mu}^*)$ show almost no difference. However, we observe a difference between the reduced and exact dual solutions $\lambda(\boldsymbol{\mu}^*)$ and $\lambda_N(\boldsymbol{\mu}^*)$. This is quantified by introducing the error measures $e_u(\boldsymbol{\mu}) := \|u(\boldsymbol{\mu}) - u_N(\boldsymbol{\mu})\|_V$ and $e_\lambda(\boldsymbol{\mu}) := \|\lambda(\boldsymbol{\mu}) - \lambda_N(\boldsymbol{\mu})\|_W$ and evaluating $e_u(\boldsymbol{\mu}^*) = 0.031626$ and $e_\lambda(\boldsymbol{\mu}^*) = 0.002891$ corresponding to the norms $\|u(\boldsymbol{\mu}^*)\|_V = 1.749663$ and $\|\lambda(\boldsymbol{\mu}^*)\|_W = 0.126907$. Note that in particular with $\alpha(\boldsymbol{\mu}^*) = 0.075$, $\beta_N = 1$, $\gamma_a(\boldsymbol{\mu}^*) = 0.15$, and $\|r\|_V = 10^{-14}$ the inequality (4.9) can be verified numerically. We illustrate examples of vectors spanning the reduced space V_N and the cone M_N in Figure 6.2. We observe that the supremizers are piecewise linear outside the support of the corresponding dual snapshots.

6.2. Efficiency of the method. We want to quantify the efficiency of our method with respect to different aspects. We first consider Model I and investigate the error decay with growing number of snapshots N_S. For this, we construct reduced
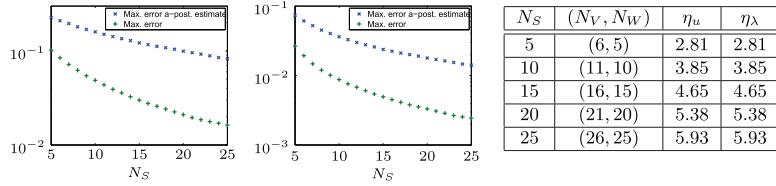
N_S	(N_V, N_W)	η_u	η_λ
5	$(6, 5)$	2.81	2.81
10	$(11, 10)$	3.85	3.85
15	$(16, 15)$	4.65	4.65
20	$(21, 20)$	5.38	5.38
25	$(26, 25)$	5.93	5.93

FIG. 6.3. *Relative errors* $\max_{\boldsymbol{\mu} \in \mathcal{F}} \left(e_u(\boldsymbol{\mu}) / \|u(\boldsymbol{\mu})\|_V \right)$ *and the corresponding relative a posteriori estimators* $\max_{\boldsymbol{\mu} \in \mathcal{F}} \left(\Delta_u(\boldsymbol{\mu}) / \|u(\boldsymbol{\mu})\|_V \right)$ *(left) and* $\max_{\boldsymbol{\mu} \in \mathcal{F}} \left(e_\lambda(\boldsymbol{\mu}) / \|\lambda(\boldsymbol{\mu})\|_W \right)$ *and* $\max_{\boldsymbol{\mu} \in \mathcal{F}} \left(\Delta_\lambda(\boldsymbol{\mu}) / \|\lambda(\boldsymbol{\mu})\|_W \right)$ *(middle). The numerical values are represented by green "+" for the errors and by blue "×" for the estimators. Additionally, the effectivities of the error estimators are given (right).*

bases corresponding to an equidistant choice of N_S parameters from $\mathcal{P}$. For the primal basis we include the supremizers and hence compute $V_N = V_N^{(2)}$ according to (2.5). For the dual reduced space, we choose $W_N = W_N^{(1)}$ from (2.2). For each reduced model, we determine the maximum error over a test-set $\mathcal{F}$ of 250 parameters given as the vertices of a fine uniform grid over $\mathcal{P}$. The results are depicted in Figure 6.3. This numerical example exhibits a nice decay of both the error and the error estimators with growing sample size N_S. Similar error convergence investigations can be obtained for Model II; we return to this point in section 6.3. Note also that the effectivity of the error estimators can be validated by the diagrams. The error estimators are rigorous upper bounds on the error, and only a slightly growing factor of about 6 is observed in overestimation. To quantify this we also compute the values of the effectivities $\eta_u := \max_{\boldsymbol{\mu} \in \mathcal{T}} \left(\Delta_u(\boldsymbol{\mu}) / e_u(\boldsymbol{\mu}) \right)$ and $\eta_\lambda := \max_{\boldsymbol{\mu} \in \mathcal{T}} \left(\Delta_\lambda(\boldsymbol{\mu}) / e_\lambda(\boldsymbol{\mu}) \right)$. The results are presented in the right part of Figure 6.3. Note that in the setting of Model I, it can be easily proven that $\Delta_u / e_u = \Delta_\lambda / e_\lambda$, which is reflected in the effectivities. Additionally, the table confirms the final observation in Remark 2.5 as we consistently obtain $N_V = N_W + 1$ due to $Q_f = 1$.

To highlight the effect of adding the supremizers in the definition of V_N, we compare our results with $V_N = V_N^{(1)} = \text{span}\{u(\mu_i)\}$, i.e., the space of snapshots without enrichment. In a first test, we compute for both settings the inf-sup constant β_N for various values of N_S. For Model I the bilinear form $a(\cdot, \cdot; \boldsymbol{\mu})$ is proportional to the scalar product on V and $Q_a = 1$. From Remark 2.5 it then follows that (2.5)–(2.7) yield the same space and that V_N compared to the naive choice is at most enriched by one element. The results are given in the left part of Figure 6.4. In this example, the supremizers greatly improve the stability of the method, and we verify the theoretical findings of $\beta_N \geq \beta = 1$ for $V_N = V_N^{(2)}$. Second, we compare the computational cost of the solver. Numerically, the number of iterations required to solve the reduced problem during the online-phase increases linearly with respect to N in both cases; see the right part of Figure 6.4. However, in the case of (2.4), the slope is roughly two times bigger than in the case of (2.5).

Let us emphasize that in this example the inclusion of the supremizer functions does not improve the accuracy of the reduced solutions. This may be explained by the fact that the supremizers do not necessarily represent valuable solution structure, as they are in some sense unphysical. But as indicated by Figure 6.4, the inf-sup constants and the number of iterations indeed improve by this space extension.

In a further test, we illustrate the runtime performance of our RB scheme compared to a parameterwise computation of the detailed solution. We evaluate the
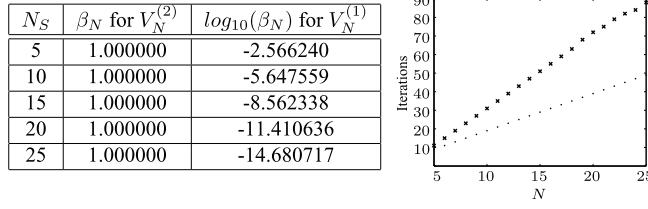
N_S	β_N for $V_N^{(2)}$	$log_{10}(\beta_N)$ for $V_N^{(1)}$
5	1.000000	-2.566240
10	1.000000	-5.647559
15	1.000000	-8.562338
20	1.000000	-11.410636
25	1.000000	-14.680717

FIG. 6.4. *Effect of the inclusion of supremizers. Inf-sup stability constants (left) and number of iterations (right) required to solve the reduced problem. Dots:* $V_N = V_N^{(2)}$ *with supremizers (cf. (2.5)); crosses:* $V_N = V_N^{(1)}$ *without supremizers (cf. (2.4)).*

TABLE 6.1
Runtime measurements for Model I *and different basis sizes, with and without enrichment.*

With supremizer enrichment, $V_N^{(2)}$

N_S	(N_V, N_W)	t_1	t_2	t_3	t_4	t_1/t_3
5	$(6,5)$	0.095526	0.546222	0.001124	0.002127	85.024714
15	$(16,15)$	0.095572	1.419460	0.004866	0.002129	19.642336
25	$(26,25)$	0.095515	2.377407	0.017057	0.002133	5.599830

Without supremizer enrichment, $V_N^{(1)}$

N_S	(N_V, N_W)	t_1	t_2	t_3	t_4	t_1/t_3
5	$(5,5)$	0.095435	0.455741	0.000887	0.002130	107.641048
15	$(15,15)$	0.095780	1.422013	0.007579	0.002149	12.637447
25	$(25,25)$	0.095320	2.371007	0.028424	0.002129	3.353503

actual acceleration due to our RB method, we measure the respective computation times of the offline- and online-phases, and we compare them to the time required by a standard method. More precisely, we define the following:

- t_1: Computation time for one fine scale solution, i.e., time required to determine $(u(\boldsymbol{\mu}_i), \lambda(\boldsymbol{\mu}_i))$. This time is closely related to the performance of the primal-dual active set strategy and depends on the dimensions of V and W.
- t_2: Offline-phase computation time, i.e., time corresponding to the snapshot computation, determination of the supremizers, the orthogonal basis $(\varphi_i)_{i=1}^{N_V}$, the matrix components $\overline{A}_N^q$ and $\overline{B}_N$, and the vector components $\overline{f}_N^q$ and $\overline{g}_N^q$.
- t_3: Online-phase computation time, i.e., time required to assemble the matrix $\overline{A}_N(\boldsymbol{\mu})$ and vectors $\overline{f}_N(\boldsymbol{\mu})$ $\overline{g}_N(\boldsymbol{\mu})$ and to solve the reduced saddle point problem in order to determine $(u_N(\boldsymbol{\mu}), \lambda_N(\boldsymbol{\mu}))$.
- t_4: Runtime for evaluation of the a posteriori error estimators.

We present average time measurements over 150 runs for Model I and different basis sizes in Table 6.1. The last column corresponds to the asymptotic speedup obtained when dealing with a large number L of simulations, i.e., $\frac{L \cdot t_1}{t_2 + L \cdot t_3} \approx \frac{t_1}{t_3}$. We see the advantage of the RB scheme in a clear acceleration. The a posteriori error estimators are also considerably cheaper than a full detailed solution, as can be seen in the large ratio of t_1/t_4. Note that the reduction of the number of solver iterations by using supremizers leads to an improved runtime, although the space extension gives rise to larger reduced problems. We conclude that the use of supremizers is an option for a guaranteed stable scheme, but does not necessarily imply an accuracy improvement. Not using supremizers may be a practical option which still gives good results, though without stability guarantee.
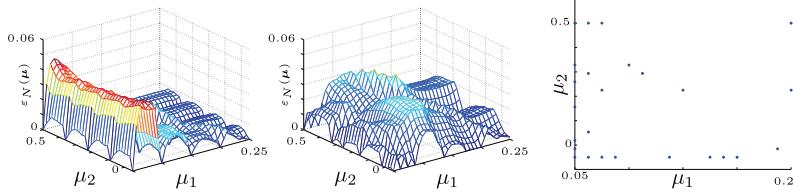
FIG. 6.5. *Numerical values of the error $\varepsilon_N(\boldsymbol{\mu}) = e_u(\boldsymbol{\mu}) + e_\lambda(\boldsymbol{\mu})$ over the fine test grid $\mathcal{F}$ when using the reduced basis $\mathcal{B}_u$ obtained by a uniform coarse grid (left) and $\mathcal{B}_\Delta$ from Algorithm 1 (middle). The selected values of the extension parameters in parameter space are indicated (right).*

6.3. RB generation with the greedy algorithm. In a last test, we use the greedy algorithm [24, 7, 11, 6, 3] for adaptive basis generation based on the a posteriori estimators Δ_u and Δ_λ described in section 4 to compute a relevant basis. In this procedure, we sequentially enrich the current basis with the snapshot corresponding to the parameter value that maximizes an error indicator $\Delta(\boldsymbol{\mu})$, e.g., $\Delta(\boldsymbol{\mu}) := \omega_u \Delta_u + \omega_\lambda \Delta_\lambda$ with some weights $\omega_u, \omega_\lambda \in \mathbb{R}^+$. The algorithm reads as follows.

ALGORITHM 1. *Input: $N_{max} \in \mathbb{N}$, accuracy ε_{tol}, initial sample $\boldsymbol{\mu}_1$, training set $\mathcal{T} \subset \mathcal{P}$.*

1. *set $k := 0$*
2. *repeat*
    (a) *set $k := k + 1$*
    (b) *compute the snapshot $(u(\boldsymbol{\mu}_k), \lambda(\boldsymbol{\mu}_k))$*
    (c) *define V_N and M_N corresponding to the snapshots $\{(u(\boldsymbol{\mu}_i), \lambda(\boldsymbol{\mu}_i))\}_{i=1}^k$*
    (d) *define $\varepsilon := \max_{\boldsymbol{\mu} \in \mathcal{T}} \Delta(\boldsymbol{\mu})$ and $\boldsymbol{\mu}_{k+1} := \arg\max_{\boldsymbol{\mu} \in \mathcal{T}} \Delta(\boldsymbol{\mu})$*
3. *until $\varepsilon < \varepsilon_{tol}$ or $k \geq N_{max}$*
4. *set $N_S := k$ and return reduced bases $\{\varphi_i\}_{i=1}^{N_V}$ and $\{\xi_i\}_{i=1}^{N_W}$.*

Only N_S detailed problems are solved (during step 2(b)). Additional manipulations of high-dimensional vectors are done only in step 2(c) to compute the supremizers and the orthogonal basis and in step 2(d) when computing the projection π required to evaluate the a posteriori estimator $\omega_u \Delta_u(\boldsymbol{\mu}) + \omega_\lambda \Delta_\lambda(\boldsymbol{\mu})$. In our case $V' = W$, and this projection consists in applying a componentwise minimum; cf. section 5.2. All other computational steps involve reduced problems typically of small dimension.

In our test, we use Model II, as a higher-dimensional parameter space promises more interesting parameter dependence. As initial value, we set $\boldsymbol{\mu}_1 = (0.15, 0.225)^T$, which is the center value of the parameter rectangle. We set the weights for the error estimator $\Delta(\boldsymbol{\mu})$ as $\omega_u = \omega_\lambda = 1$. We compare the following different basis generation procedures. The reduced basis associated with the coarse grid $\mathcal{C}$ of $5 \times 5 = 25$ uniformly distributed points in $\mathcal{P}$ is denoted by $\mathcal{B}_u$. Further, $\mathcal{B}_\Delta$ stands for the reduced basis resulting from Algorithm 1 using the a posteriori error estimator $\Delta(\boldsymbol{\mu})$ with $N_{max} = 25$. The training grid $\mathcal{T}$ we use is composed of $17 \times 17 = 289$ uniformly distributed points. The basis obtained by the greedy algorithm using the true error as selection measure, i.e., $\Delta(\boldsymbol{\mu})$ is replaced with $\varepsilon_N(\boldsymbol{\mu}) := \omega_u e_u(\boldsymbol{\mu}) + \omega_\lambda e_\lambda(\boldsymbol{\mu})$, is denoted by $\mathcal{B}_e$. The latter basis generation procedure is computationally expensive for high-dimensional problems, but it is included as a reference method. In all cases we obtain $N_S = 25$ snapshots and determine the error ε_N on a fine test grid $\mathcal{F}$ of $33 \times 33 = 1089$ uniformly distributed points. The results are depicted in Figure 6.5. We observe that the error for training samples indeed is zero; see Propositions 3.1 and 4.4. The greedy procedure results in overall lower errors, in particular for the low μ_1 value range, as it is able to adaptively locate snapshots in this critical region.

TABLE 6.2
Size of basis and maximal test errors obtained when using the greedy algorithm or a uniform grid.

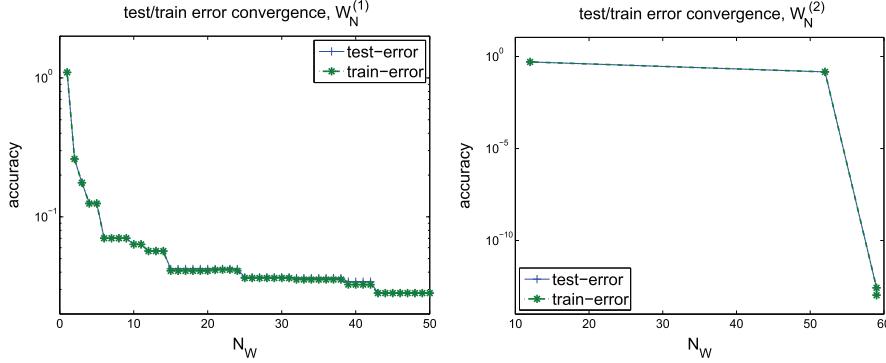|	$\max_{\boldsymbol{\mu}\in\mathcal{F}}\{e_u\}$	$\max_{\boldsymbol{\mu}\in\mathcal{F}}\{e_\lambda\}$	$\max_{\boldsymbol{\mu}\in\mathcal{F}}\{\varepsilon_N\}$	N_V
$\mathcal{B}_u$	0.042473	0.003961	0.045450	32
$\mathcal{B}_\Delta$	0.031988	0.004795	0.036783	42
$\mathcal{B}_e$	0.018440	0.002513	0.020471	41

FIG. 6.6. *Evolution of test error* $\max_{\boldsymbol{\mu}\in\mathcal{F}}\{\varepsilon_N\}$ *(blue crosses) and train error* $\max_{\boldsymbol{\mu}\in\mathcal{T}}\{\varepsilon_N\}$ *(green stars) for greedy basis* $\mathcal{B}_\Delta$ *using* $W_N^{(1)}$ *(left) and* $W_N^{(2)}$ *(right).*

The maximal error ε_N and its components e_u, e_λ are significantly reduced, which is shown in Table 6.2.

In this example, the accuracy $\varepsilon_N = 0.045450$ is obtained using the uniform grid $\mathcal{C}$ with $N_S = 25$ snapshots and a reduced primal space of dimension $N_V = 32$. When using the greedy algorithm with the a posteriori error estimators, the same accuracy is obtained with $N_S = 18$ snapshots, and the corresponding basis $\mathcal{B}_\Delta$ contains in this case $N_V = 35$ vectors. The a posteriori error estimators indeed seem to be good substitutes for the true errors in the greedy algorithm.

The pictures in Figure 6.6 show the benefits of the choices $W_N^{(1)}$ and $W_N^{(2)}$. We plot the decrease of the maximum error ε_N over the train and test-set along the iterations of the construction of $\mathcal{B}_\Delta$. Note that a model with error $O(10^{-1})$ in this example is to be considered as practically good; cf. the example error values in section 6.1. While the first curve using $W_N^{(1)}$ is within the spirit of RB techniques and is thus very attractive from the computational point of view of solving low-dimensional systems, it may result in a reduced convergence rate for larger dimensions. On the other hand, the second approach $W_N^{(2)}$ yields extremely good approximation properties but may yield large systems to solve; cf. Remark 2.2. The four indicated points correspond to $(N_S, N_W, N_V) = (1, 12, 13), (2, 52, 54), (3, 59, 62), (4, 59, 63)$, and hence each of the few greedy extension steps increases N_W (and N_V) considerably, as all detailed basis vectors are selected that belong to the support of the snapshots. We expect $W_N^{(2)}$ to work well in case of, e.g., contact problems in two or three space dimensions, where the Lagrange multiplier space is associated only with the boundary of the computational domain. Then, the finite element space dimension H_W, and herewith N_W, is guaranteed to be much smaller than H_V. Procedures combining the good error convergence of $W_N^{(2)}$ with the low dimension increase of $W_N^{(1)}$ will be the subject of further investigation. Overall, the results indicate that the greedy algorithm is a procedure leading to compact bases, also in our case of variational inequalities.

B. HAASDONK, J. SALOMON, AND B. WOHLMUTH

REFERENCES

[1] M. AINSWORTH, J. ODEN, AND C. LEE, *Local a posteriori error estimators for variational inequalities*, Numer. Methods Partial Differential Equations, 9 (1993), pp. 23–33.
[2] M. BARRAULT, Y. MADAY, N. C. NGUYEN, AND A. T. PATERA, *An "empirical interpolation" method: Application to efficient reduced-basis discretization of partial differential equations*, C. R. Math. Acad. Sci. Paris, 339 (2004), pp. 667–672.
[3] P. BINEV, A. COHEN, W. DAHMEN, R. DEVORE, G. PETROVA, AND P. WOJTASZCZYK, *Convergence rates for greedy algorithms in reduced basis methods*, SIAM J. Math. Anal., 43 (2011), pp. 1457–1472.
[4] V. BOSTAN, W. HAN, AND B. REDDY, *A posteriori error estimation and adaptive solution of elliptic variational inequalities of the second kind*, Appl. Numer. Math., 52 (2005), pp. 13–38.
[5] F. BREZZI AND M. FORTIN, *Mixed and Hybrid Finite Element Methods*, Springer, New York, 1991.
[6] A. BUFFA, Y. MADAY, A. T. PATERA, C. PRUD'HOMME, AND G. TURINICI, *A priori convergence of the greedy algorithm for the parametrized reduced basis method*, ESAIM Math. Model. Numer. Anal., 46 (2012), pp. 595–603.
[7] J. L. EFTANG, A. T. PATERA, AND E. M. RØNQUIST, *An "hp" certified reduced basis method for parametrized elliptic partial differential equations*, SIAM J. Sci. Comput., 32 (2010), pp. 3170–3200.
[8] I. EKELAND AND R. TEMAM, *Convex Analysis and Variational Problems*, Stud. Math. Appl. 1, North–Holland, Amsterdam, 1976.
[9] R. GLOWINSKI, *Numerical Methods for Variational Problems*, Springer, Berlin, 2008.
[10] M. A. GREPL AND A. T. PATERA, *A posteriori error bounds for reduced-basis approximations of parametrized parabolic partial differential equations*, M2AN Math. Model. Numer. Anal., 39 (2005), pp. 157–181.
[11] B. HAASDONK, M. DIHLMANN, AND M. OHLBERGER, *A training set and multiple bases generation approach for parametrized model reduction based on adaptive grids in parameter space*, Math. Comput. Model. Dyn, Syst., 17 (2011), pp. 423–442.
[12] B. HAASDONK AND M. OHLBERGER, *Reduced basis method for finite volume approximations of parametrized linear evolution equations*, M2AN Math. Model. Numer. Anal., 42 (2008), pp. 277–302.
[13] C. HAGER AND B. WOHLMUTH, *Semismooth Newton methods for variational problems with inequality constraints*, GAMM-Mitt., 33 (2010), pp. 8–24.
[14] K. ITO AND K. KUNISCH, *Lagrange Multiplier Approach to Variational Problems and Applications*, SIAM, Philadelphia, 2008.
[15] T. KARKKAINNEN, K. KUNISCH, AND P. TARVAINEN, *Primal-dual active set methods for obstacle problems*, J. Optim. Theory Appl., 119 (2003), pp. 499–533.
[16] D. KINDERLEHRER and G. STAMPACCHIA, *An Introduction to Variational Inequalities and Their Applications*. SIAM, Philadelphia, 2000.
[17] A. E. LØVGREN, Y. MADAY, AND E. M. RØNQUIST, *A reduced basis element method for the steady Stokes problem*, M2AN Math. Model. Numer. Anal., 40 (2006), pp. 529–552.
[18] R. A. NICOLAIDES, *Existence, uniqueness and approximation for generalized saddle point problems*, SIAM J. Numer. Anal., 19 (1982), pp. 349–357.
[19] D. V. ROVAS, *Reduced-Basis Output Bound Methods for Parametrized Partial Differential Equations*, Ph.D. thesis, MIT, Cambridge, MA, 2003.
[20] D. V. ROVAS, L. MACHIELS, AND Y. MADAY, *Reduced basis output bound methods for parabolic problems*, IMA J. Numer. Anal., 26 (2006), pp. 423–445.
[21] G. ROZZA, *Shape Design by Optimal Flow Control and Reduced Basis Techniques: Applications to Bypass Configurations in Haemodynamics*, Ph.D. thesis, École Polytechnique Fédérale de Lausanne, Switzerland, 2005.
[22] G. ROZZA, D. B. P. HUYNH, AND A. T. PATERA, *Reduced basis approximation and a posteriori error estimation for affinely parametrized elliptic coercive partial differential equations: Application to transport and continuum mechanics*, Arch. Comput. Methods Eng., 15 (2008), pp. 229–275.
[23] G. ROZZA AND K. VEROY, *On the stability of the reduced basis method for Stokes equations in parametrized domains*, Comput. Methods. Appl. Mech. Engrg., 196 (2007), pp. 1244–1260.
[24] K. VEROY, C. PRUD'HOMME, D. V. ROVAS, AND A. T. PATERA, *A posteriori error bounds for reduced-basis approximation of parametrized noncoercive and nonlinear elliptic partial differential equations*, in Proceedings of the 16th AIAA Computational Fluid Dynamics Conference, 2003, Paper. 2003-3847.